Eur. J. Mineral., 37, 617–626, 2025
https://doi.org/10.5194/ejm-37-617-2025

European Journal of Mineralogy
Open Access

Chromites in ordinary-chondrite fusion crusts

Manlio Bellesi[1,†], Giovanni Pratesi[2], Alessandro Di Michele[3], Sabrina Nazzareni[4], Lidia Pittarello[5,6], Steven Goderis[7], Carlo Santini[1], and Gabriele Giuli[8]

[1]School of Science and Technology – chemistry division, University of Camerino, Via Madonna delle carceri (ChIP), 62032 Camerino, Italy
[2]Dipartimento di Scienze della Terra, Università di Firenze, Via G. La Pira 4, 50121 Firenze, Italy
[3]Dipartimento di Fisica e Geologia, Università di Perugia, Via Pascoli, 06100, Perugia, Italy
[4]Dipartimento di Scienze Chimiche, della Vita e della Sostenibilità Ambientale, Università di Parma, Parco Area delle Scienze 157/A, 43124, Parma, Italy
[5]Naturhistorisches Museum Wien, Mineralogisch-Petrographische Abteilung, Burgring 7, 1010 Vienna, Austria
[6]Department of Lithospheric Research, University of Vienna, Althanstrasse 14, 1090 Vienna, Austria
[7]Archaeology, Environmental Changes, and Geo-Chemistry (AMGC), Vrije Universiteit Brussel (VUB), Pleinlaan 2, 1050 Brussels, Belgium
[8]School of Science and Technology – geology division, University of Camerino, Via Gentile III da Varano, 7, 62032 Camerino, Italy
†deceased

Correspondence: Gabriele Giuli (gabriele.giuli@unicam.it)

Received: 28 February 2025 – Revised: 12 June 2025 – Accepted: 18 June 2025 – Published: 10 September 2025

Abstract. Chromites from ordinary chondrites of groups H4, H5, LL5, LL6, L3.6 and L6 were studied and compared to an H5 ordinary chondrite processed to form a synthetic fusion crust. Chromites found in the bulk are usually anhedral and relatively large in size (several tens of micrometres), as opposed to chromites formed within the crust, which are consistently smaller (a few micrometres in size) and can display anhedral or subhedral to euhedral habit.

The Mg# and Al# values of the chromites in the bulk display typical composition reported for ordinary chondrites, with a limited scatter of Al# (ca. 0.13 ± 0.025) but a large variation in Mg# (from 0.05 to 0.30).

Chromites within fusion crusts generally exhibit similar Al# values with respect to those in the bulk but a much larger scatter of Mg# values and a larger average Mg# (up to 0.65).

Chromites in the fusion crusts are often associated with magnetite dendrites made up of magnetite octahedral crystals that are 100–400 nm wide; occasionally, other spinel group minerals can be found, such as magnesiochromites and magnesioferrites. In most of the studied samples, several chromite crystals are mantled by magnetite crystals. Textural data collected so far suggest a crystallisation sequence in the fusion crust, starting with olivine and going over chromite to magnetite.

A small but significant fraction (~ 15 %) of chromites grown in the fusion crust display a detectable Ni content, in marked contrast with those found in the bulk, where only ca. 2 % of the analysed chromites display Ni contents above the detection limit.

These observations are additionally supported by measurements on the El Hammami (H5) meteorite sample, which was previously processed with an induction-heated plasma wind tunnel in order to create a synthetic fusion crust. Also in this case, chromites found within the fusion crust formed under controlled conditions (temperature measured at the sample surface at 2400–2200 K for 20 s) display similar Al# and considerably higher Mg# compared to those in the bulk, which is similar to the chromites in the natural fusion crusts studied here. Our study shows that chromites of meteoritic origin retrieved from sediment can display significantly higher Mg# values than those of the parent meteoroid if they originate within the fusion crust, providing a way to recognise chromites from ablation spherules.

1 Introduction

Spinel group minerals are accessory phases in many chondrite meteorites, the most common term being chromite in ordinary chondrites. In addition, some highly oxidised type 3 chondrites also contain magnetite (e.g. Taylor and Brownlee, 1991). Chromites in ordinary chondrites are usually solid solutions between chromite ($FeCr_2O_4$), magnesiochromite ($MgCr_2O_4$), spinel ($MgAl_2O_4$) and hercynite ($FeAl_2O_4$), where minor substitution of V and Ti for Cr and Al and of Mn and Zn for Fe and Mg can occur.

Chromite composition may be expressed by $Mg\# = Mg/(Mg + Fe)$ and $Al\# = Al/(Al + Cr)$. A systematic study of chromite composition in ordinary-chondrite meteorites (Wlotzka, 2005; Ramdohr, 1967; Bunch et al., 1967) showed values of Al# close to 0.14 and Mg# varying in a range between 0.09 (LL samples) and 0.17 (H samples), with an average value of 0.13 for the L samples (Wlotzka, 2005). In particular, Mg# seems to correlate with the ordinary-chondrite class, with LL group usually having lower Mg# than L and H groups.

The TiO_2 content of chromites can be used to determine the meteorite class for extraterrestrial chromite grains found in sediments and fossil meteorites (Schmitz et al., 2017). Fossil meteorites refer to the recognisable remnants of meteorites fallen on Earth in the past – of which only a handful of specimens have been identified (see, for instance, Schmitz and Tassinari, 2001).

The purpose of this work is to carry out a systematic comparison between chromites found in the bulk of ordinary chondrites and those forming within the fusion crust during the meteoroid's passage through the Earth's atmosphere. These data may help in understanding the outcomes of meteorite fusion experiments (see Helber et al., 2019, and Pittarello et al., 2019, for experimental conditions and sample characterisation) and potentially contribute to a deeper understanding of the formation and evolution of meteorite melt during the ablation stage, which is scarcely documented in the literature.

2 Samples and experimental approach

We selected 10 ordinary chondrites with well-preserved fusion crusts:

- two from the LL group (Chelyabinsk LL5, Kilabo LL6),
- three from the L group (Aba Panu L3.6, Viñales L6, NWA869 L3-6),
- five from the H group (Bassikounou H5, Chergach H5, Kabo H4, Tamdakht H5, El Hammami H5).

El Hammami (H5) is an H-type ordinary chondrite used by Pittarello et al. (2019) to reproduce a fusion crust in the laboratory. Pittarello et al. (2019) experimentally melted El Hammami sample by an induction-heated plasma wind tunnel at the von Karman Institute for Fluid Dynamics in Rhode-Saint-Genèse, Belgium. The experiment was conducted under known plasma temperature and velocity conditions (see Helber et al., 2019, for details). The surface temperature of the meteorite was measured during the melting experiment, and after the synthetic fusion crust was recovered, it was petrographically and geochemical characterised (Pittarello et al., 2019).

All the meteorites here considered are falls, except El Hammami and NWA869, which are finds. We selected fall meteorites, whenever available, due to their lower degree of terrestrial alteration compared to find meteorites.

Preliminary meteorite characterisation was performed by optical microscopy, followed by imaging and in situ microchemical chromite characterisation by field-emission scanning electron microscopy (FE-SEM) on petrographic thin sections (ca. 30 µm thickness). Microchemical compositional data have been measured by means of FE-SEM at the School of Science and Technology (University of Camerino) and at the Department of Physics and Geology (University of Perugia).

The Sigma300 Zeiss FE-SEM (University of Camerino) is equipped with three electron detectors: an "in-lens" secondary electron detector, an Everhart–Thornley secondary electron detector and a four-sector high-definition backscattered electron detector. X-rays emitted by the samples have been analysed by a Bruker Qantax 200 silicon drift detector (SDD), with a 129 eV resolution at the Mn $K\alpha$ emission line.

The LEO 1525 Zeiss FE-SEM (University of Perugia) is equipped with a an AsB (angle-selective back-scattered) back-scattered electron detector, an in-lens secondary electron detector and a Bruker Quantax 200 energy-dispersive X-ray (EDX) detector (equipped with an X-Flash 410 detector).

In both instruments, FE-SEM measurements were operated at 15 kV with a working distance of 8 mm. Espirit 1.9 software using ZAF correction has been used to derive elemental abundances after calibration with reference materials.

Details on the accuracy of chemical compositional data acquired by FE-SEM instruments with respect to electron probe micro-analyser (EPMA) data on the same standards can be found in the Supplement.

Multiple analyses on synthetic material or material previously characterised by EPMA allowed us to ascertain that, for the composition of olivine, pyroxene and chromite, the relative error (1σ) for major elements is in the 5 % to 6 % range, whereas the relative error for minor elements (e.g. Ti in chromite) is in the 10 %–12 % range. The determination of V is highly affected by the presence of Ti because of the overlapping of the Ti $K\alpha$ emission line with the V $K\beta$ emis-

sion line, resulting in a much larger error. The same applies for Mn (whose $K\alpha$ emission line overlaps with the Cr $K\beta$ emission line).

Compositional data have been provided by the Esprit program in mole percent of atoms after ZAF correction. The compositions have been normalised by constraining the sum of the cations to 3.0 atoms per formula unit (p.f.u.). By applying this normalisation procedure, the sum of the cations supposedly located in the tetrahedral site (mostly Fe^{2+} and Mg) results, with only a few exceptions, in values close to 1.0 within the reported error, whereas the sum of the cations supposedly located in the octahedral site (Cr, Al, Ti, V) results in values close to 2.0. The few exceptions (mostly for chromite within the fusion crust) will be discussed separately.

A calculation of the equilibrium relations among the phases present in the crust was tentatively carried out using easyMELTS software (Ghiorso and Sack, 1995; Smith and Asimow, 2005).

We assumed an $fO2$ value starting from the measured $Fe^{3+}/(Fe^{2+}+Fe^{3+})$ ratio of the glass formed from the melted basalt ranging between 0.15 and 0.17. After several attempts, a QFM+1 buffer was used in the calculations, as it better reproduced the $Fe^{3+}/(Fe^{2+}+Fe^{3+})$ ratio measured in a glass produced with the induction-heated plasma wind tunnel under the same conditions as were used to create a synthetic fusion crust with mineralogy and texture comparable to natural fusion crusts (Pittarello et al., 2019). Isothermal crystallisation was carried out to calculate the crystallisation sequence after the calculation of liquidus temperature at 1 atm pressure. We calculated the isothermal crystallisation from the liquidus temperature with 20 °C steps at fixed pressure of 1 atm down to 500 °C to evaluate the complete crystallisation.

3 Results

We obtained compositional data for 309 chromites: 150 chromites from the interior of the meteorite samples and 159 chromites from their respective fusion crusts. The chromites studied here are distributed as follow: 105 for H chondrites, 157 for L chondrites and 47 for LL chondrites. Detailed data are reported in the Supplement (Table S2).

Chromites reported here are mostly "coarse chromite" as defined by Ramdohr (1973), mainly anhedral and with sizes up to several tens to hundreds of micrometres (Fig. 1a–d). However, chromites found in plagioclase–chromite assemblages (as described by Rubin, 2003) have smaller sizes (usually less than 15 µm) and euhedral habit; only 2 chromites in Tamdakht and 2 in Viñales from chromite–plagioclase assemblages have been analysed here. No chromite-bearing type II chondrules have been found in the studied samples. Chromites in the fusion crust (Fig. 1e–f) are predominantly less than 10 µm in size and exhibit subhedral to euhedral habit.

Most of the chromites in the meteorite interior display Al/(Al + Cr) close to 0.14; only chromites within the plagioclase–chromite assemblages have higher values of Al/(Al + Cr) ratios (up to 0.27). The Mg/(Mg + Fe) ratio varies between 0.09 and 0.56. The standard deviations for Al/(Al + Cr) and Mg/(Mg + Fe) ratios of the chromites in the meteorite interior are on average low (0.038 average for Al# and 0.043 average for Mg#).

Composition of chromites in the fusion crusts, on the other hand, can display large differences with respect to chromites in the interior. Al# varies between 0.09 and 0.17, similarly to chromites in the interior (Table 1). Mg# has larger standard deviations compared to those in the interior (0.126 average compared to 0.043 average) and higher absolute values, in some cases plotting in the field of Mg-chromite composition (Mg# > 0.5).

In a few cases, we encountered normalised chromite compositions in the fusion crust in which the sum of Mg + Fe significantly exceeded 1 (and, correspondingly, the sum of Al + Cr + Ti + V was significantly lower than 2). We suggest that this could be the result of small amounts of Fe^{3+} located in the octahedral site. The presence of small but significant amounts of Fe^{3+} in the fusion crusts is consistent with experimental data on basalt melted under the same conditions as a natural meteorite (Pittarello et al., 2019), using an induction-heated plasma wind tunnel to tentatively mimic the conditions of an incoming meteoroid. In the Pittarello et al. (2019) experiment, the $Fe^{3+}/(Fe^{2+}+Fe^{3+})$ ratio of the glass formed from the melted basalt ranged between 0.15 and 0.17. These values are consistent with the formation of small amounts of magnetite in the silicate melt and with a possible magnetite component in the chromite formed within a melted portion of a meteorite. The difference in the Mg# between chromites in the interior and those in the crust is generally pronounced. Plotting Al# vs. Mg# for bulk and crust chromites (Fig. 2a, b, c), it is evident that bulk chromites exhibit smaller standard deviations, whereas the Mg# of crust chromites exhibits significantly greater scatter and, consequently, a larger standard deviation. As a consequence, plotting Al# and Mg# average values (filled symbols in Figs. 2 and 3), crust chromite major chemistry appears to be significantly different to that of bulk chromites, with larger Mg# values on average.

The studied chromites contain minor amounts of Ti and Ni, with their abundances differing significantly between chromites formed in the fusion crust and those in the bulk.

Although the measurement of Ti is affected by a larger error than that of Mg, a meaningful trend can be discussed using the average TiO_2 content. The TiO_2 content of bulk chromites (Table S1, Supplement) plots within the ranges reported by Schmitz et al. (2017) for different ordinary-chondrite classes, with only two exceptions: (1) Chelyabinsk bulk chromites have an average TiO_2 content (2.93 wt %) that is slightly lower than that of the LL chondrites reported in the literature, usually ranging between 3.50 and 4.50 wt %, and (2) Kabo bulk chromites have a slightly higher average TiO_2

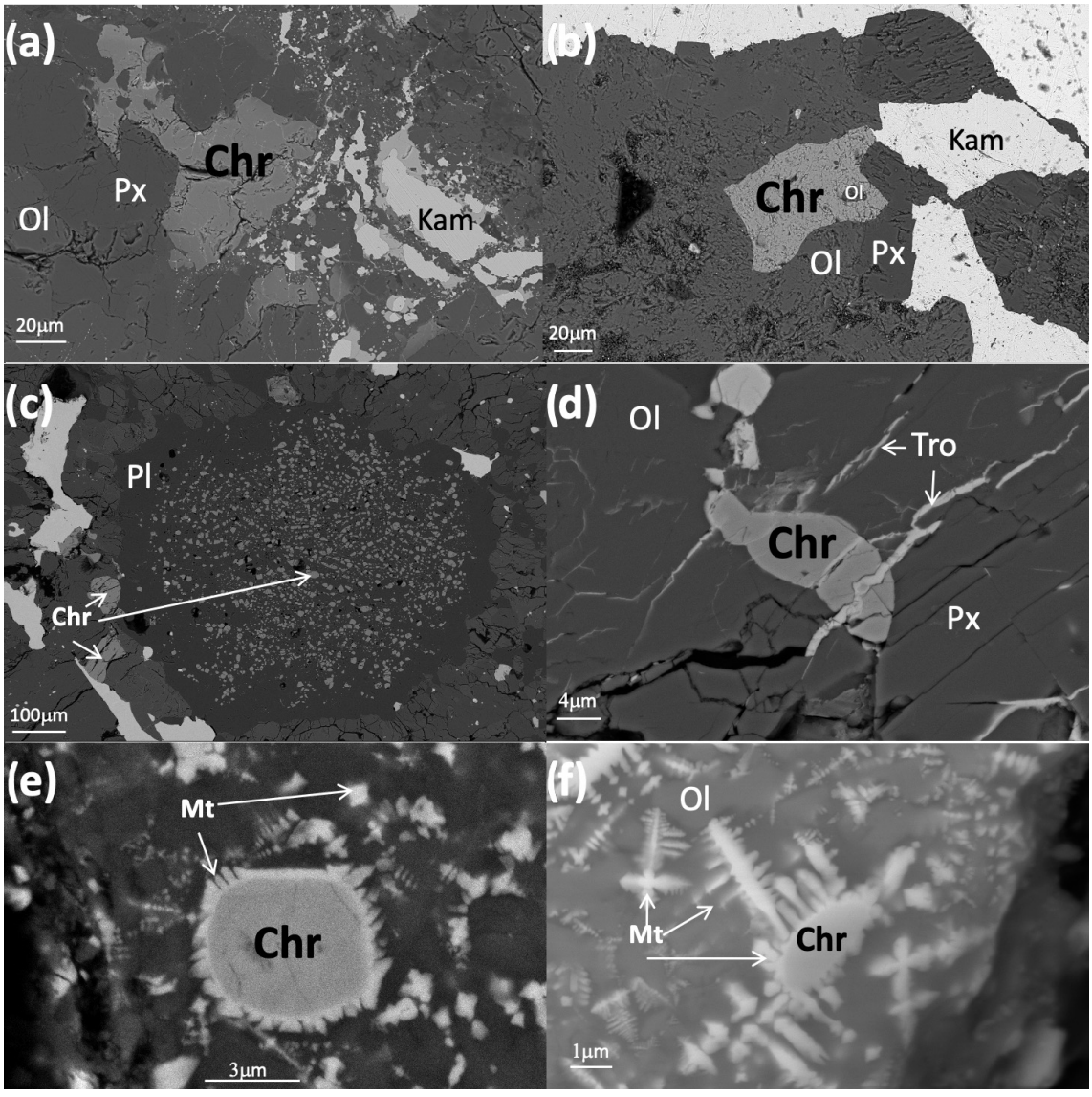

Figure 1. Common occurrences of chromite grains in the ordinary chondrites studied: **(a)** large anhedral chromite (Chr) occurring together with forsterite (Ol), enstatite (Px) and kamacite (Kam) within the Aba Panu L3.6 chondrite; **(b)** large anhedral chromite (Chr) occurring together with forsterite (Ol) and enstatite (Px) within the Chelyabinsk LL5 chondrite; **(c)** chromite (Chr)–plagioclase (Pl) assemblage consisting of many small euhedral to subhedral chromite crystals embedded within a plagioclase grain in the Viñales L6 chondrite; **(d)** large anhedral chromite grain intersected by troilite (Tro) veins in the outer substrate of the Viñales L6 chondrite; **(e)** small subhedral chromite grain overgrown by magnetite (Mt) nano- to micro-crystalline dendrites within the fusion crust of the Kilabo L6 chondrite; **(f)** small rounded chromite grain overgrown by magnetite nanocrystalline dendrites within the fusion crust of the Chergach H5 chondrite.

content (2.97 wt %) compared to chromites in H chondrites, which usually ranges between 1.50 and 2.50 wt %.

The standard deviations for the average TiO_2 content are between 0.13 and 1.55; the large error may depend on differences in TiO_2 content distribution or on large analytical error due to the low Ti content.

The TiO_2 content of chromites in the crust is lower than that in the interior. However, the difference is not as large as observed for the Mg#.

Overall, the Ni content of chromite is very low and only above the detection limit in ∼ 2 % (only 3 out of 150) of bulk chromites in the meteorite interior and in 15 % (25 out of 159) of the chromites within the fusion crusts.

To better understand chemical and textural relationships of the studied material, a sample of El Hammami meteorite previously used for a melting experiment by means of an induction-heated plasma wind tunnel (Pittarello et al., 2019) has been studied. The experiment succeeded in forming a melted crust displaying various features typical of natural

Table 1. Summary of compositional data for chromites in the meteorite interiors and within their fusion crust. "Ave" denotes average, "st. dev" denotes standard deviation and "n.d." denotes not detected.

Name	Type	Shock grade	Weathering grade	Mg# interior	Mg# crust	Al# interior	Al# crust	TiO_2 wt % interior	TiO_2 wt % crust	# analyses
				Ave (st. dev)	Ave (st. dev)	Ave (st. dev)	Ave (st. dev)	Ave (st. dev)	Ave (st. dev)	
Bassikounou	H5	S4	W0	0.192 (0.033)	0.563 (0.195)	0.157 (0.03)	0.154 (0.014)	2.34 (1.55)	1.32 (0.39)	27
Chergach	H5	S3	W0	0.212 (0.143)	0.507 (0.242)	0.193 (0.082)	0.195 (0.04)	1.76 (0.53)	1.38 (0.46)	31
Kabo	H4	–	W0	0.114 (0.013)	0.251 (0.185)	0.13 (0.006)	0.119 (0.012)	2.97 (0.25)	2.50 (1.14)	21
Tamdakht	H5	S3	W0	0.209 (0.027)	0.247 (0.098)	0.181 (0.024)	0.175 (0.019)	1.92 (0.12)	1.54 (0.45)	26
Aba Panu	L3.6	S4	W0	0.302 (0.077)	0.252 (0.092)	0.134 (0.136)	0.088 (0.043)	2.54 (1.31)	1.49 (0.59)	45
NWA869	L3-6	S3	W1	0.136 (0.021)	0.164 (0.031)	0.132 (0.017)	0.14 (0.042)	2.95 (0.52)	2.57 (0.66)	30
Viñales	L6	S3	W0	0.15 (0.033)	0.185 (0.067)	0.14 (0.046)	0.116 (0.01)	2.74 (0.52)	2.82 (0.45)	32
Chelyabinsk	LL5	S4	W0	0.134 (0.031)	0.493 (0.124)	0.17 (0.027)	0.143 (0.027)	2.93 (0.91)	3.18 (1.36)	25
Kilabo	LL6	S3	W0	0.094 (0.013)	0.198 (0.127)	0.13 (0.008)	0.165 (0.026)	3.76 (0.44)	3.11 (0.54)	22
El Hammami	H5	S2	n.d.	0.197 (0.036)	0.323 (0.102)	0.165 (0.006)	0.177 (0.008)	2.045 (0.491)	1.529 (0.387)	25

fusion crusts of ordinary chondrites: zoned skeletal to dendritic olivine crystals, small subhedral to euhedral chromite crystals and nanocrystalline magnetite dendrites.

The chemical composition of 25 chromites (15 in the bulk and 10 in the synthetic crust) resulted in a narrow distribution in Al/(Al + Cr) vs. Mg/(Mg + Fe) for the chromite from the meteorite interior, while chromites from the synthetic crust have more scattered Mg/(Mg + Fe) values (Table S1 and Fig. 4).

We used the crust composition of Chelyabinsk LL5 and Chergach H5 to calculate the crystallisation sequence using easyMELTS software (Ghiorso, and Sack 1995; Smith and Asimow, 2005).

The calculated liquidus temperatures vary from 1704 °C in Chelyabinsk to 1667 °C in Chergach. Olivine is the first solid phase in equilibrium with melt in Chergach (at 1644 °C), whereas in Chelyabinsk the first solid phase is a spinel (at 1644 °C). Chergach has some differences in the sequence of crystallisation with respect to Chelyabinsk.

For Chergach the early high-temperature crystallisation sequence is olivine $(Mg_{0.94}Fe^{2+}_{0.05}Ni_{0.01})_2SiO_4$ and Cr-spinel $(Fe^{2+}_{0.21}Mg_{0.79}\ Fe^{3+}_{0.42}\ Al_{0.33}Cr_{1.24}Ti_{0.01}O_4)$, and only when the residual liquid is around 20 % do feldspar and clinopyroxene start to crystallise at around $T = 1083$–1104 °C. Only at lower T (804 °C) does orthopyroxene start to crystallise at a residual liquid fraction of around 2 %. At 600 °C, the system is almost solid (98.65 mass of solid).

In Chelyabinsk the early high-temperature crystallisation sequence is Cr-spinel $(Fe^{2+}_{0.15}Mg_{0.86}Fe^{3+}_{0.50}Al_{0.38}Cr_{1.11}Ti_{0.01}O_4)$ and olivine $(Mg_{0.93}Fe^{2+}_{0.05}Ni_{0.01})_2SiO_4$; when the residual liquid is around 14 %–18 %, feldspar and clinopyroxene start to crystallise at around $T = 1083$–1104 °C. At 600 °C, the residual liquid is 0.65 and orthopyroxene is stable.

With decreasing temperature, spinel composition from a chromite-prevalent end-member changes to magnetite composition. In general the Mg# decreases with temperature (from 0.56 at 1544 °C to 0.11 at 1004 °C in Chergach, from 0.85 at 1644 °C to 0.25 at 1004 °C in Chelyabisk), whereas Al# increases in Chergach from 0.21 to 0.44 and in Chelyabisk from 0.26 to 0.59, decreasing T until around 1004 °C, which is when pyroxene and feldspar crystallise and then sharply decrease in both samples.

4 Discussion

In order to minimise the possible effect of terrestrial alteration on the composition and texture of the chromites, we selected a group of 10 ordinary chondrites from L, LL and H groups (Table 1). Most of the selected meteorites belong to falls that have been witnessed and recovered soon after landing.

We analysed 134 chromites in the meteorite interior and 150 chromites in the crust; after cation normalisation,

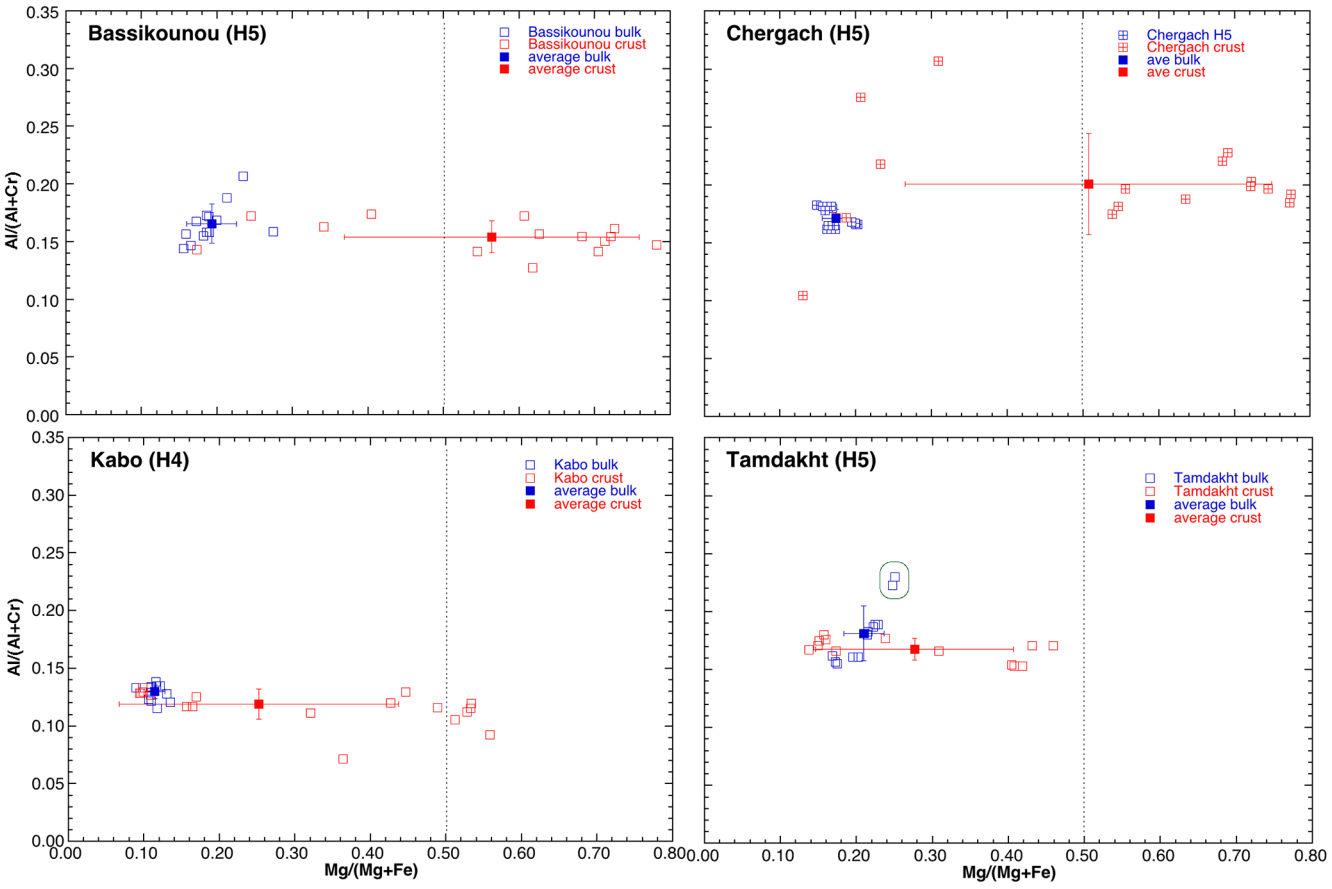

Figure 2. Al/(Al + Cr) vs. Mg/(Mg + Fe) values for chromites in the studied H chondrites. The chromites found in the fusion crust (unfilled red symbols) usually display higher Mg/(Mg + Fe) values, as well as a larger standard deviation. Filled blue and red symbols refer to the average values of the chromites in the meteorite interior and in the fusion crust. The chromites enclosed in green (Tamdakht) are not coarse chromites but small euhedral chromites within a chromite–plagioclase assemblage (Rubin, 2003).

most of the analysed chromites have a composition with Cr + Al + Ti + V summing to 2 cations p.f.u. and Fe + Mg summing to 1 cation p.f.u. The observed chemical trends between chromites from the fusion crust and the interior of the meteorites showed negligible differences between falls and finds.

In the meteorite interior, we analysed chromites with different morphological features: unfractured to fractured chromites, fractured chromites containing sulfide veins and chromite–plagioclase assemblages. In the Chelyabinsk meteorite, we found a chromite vein within plagioclase.

Chromites have a subhedral to anhedral morphology and are up to several hundred micrometres across, except chromites in the plagioclase–chromite assemblages have smaller sizes (few micrometres) and euhedral morphology.

A limited variation in the Al# (close to 0.14) has been observed for most of the bulk chromites, except chromites within the plagioclase–chromite assemblages that have higher values of Al# – as already observed by Rubin (2003). Instead Mg# varies between 0.09 and 0.56, in agreement with compositional variation reported by Ramdohr (1967), Bunch et al. (1967), Schmitz and Tassinari (2001), Rubin (2003), Wlotzka (2005), and Schmitz (2013).

According to our dataset, LL ordinary chondrites exhibit slightly lower values of Mg# compared to L and H ordinary chondrites. It is worth noting that the standard deviations of both Al# and Mg# of the bulk chromites are generally low within each meteorite.

Chromites found within the fusion crusts, differently from those in the bulk, are mostly euhedral to subhedral and display smaller sizes, from sub-micrometric to a few micrometres; we did not find chromites within the fusion crust larger than 15 µm. Size is a limit to our study, since only for chromites larger than 2–3 µm could we determine reliable compositions. For smaller crystal sizes, the interaction volume of the electrons exceeds that of the crystal, and fluorescence emission from surrounding minerals (often olivine) also markedly alters the measured Mg content. Despite this limitation, we could analyse a close-to-equity number of chromites from the crust (142) and meteorite interior (118).

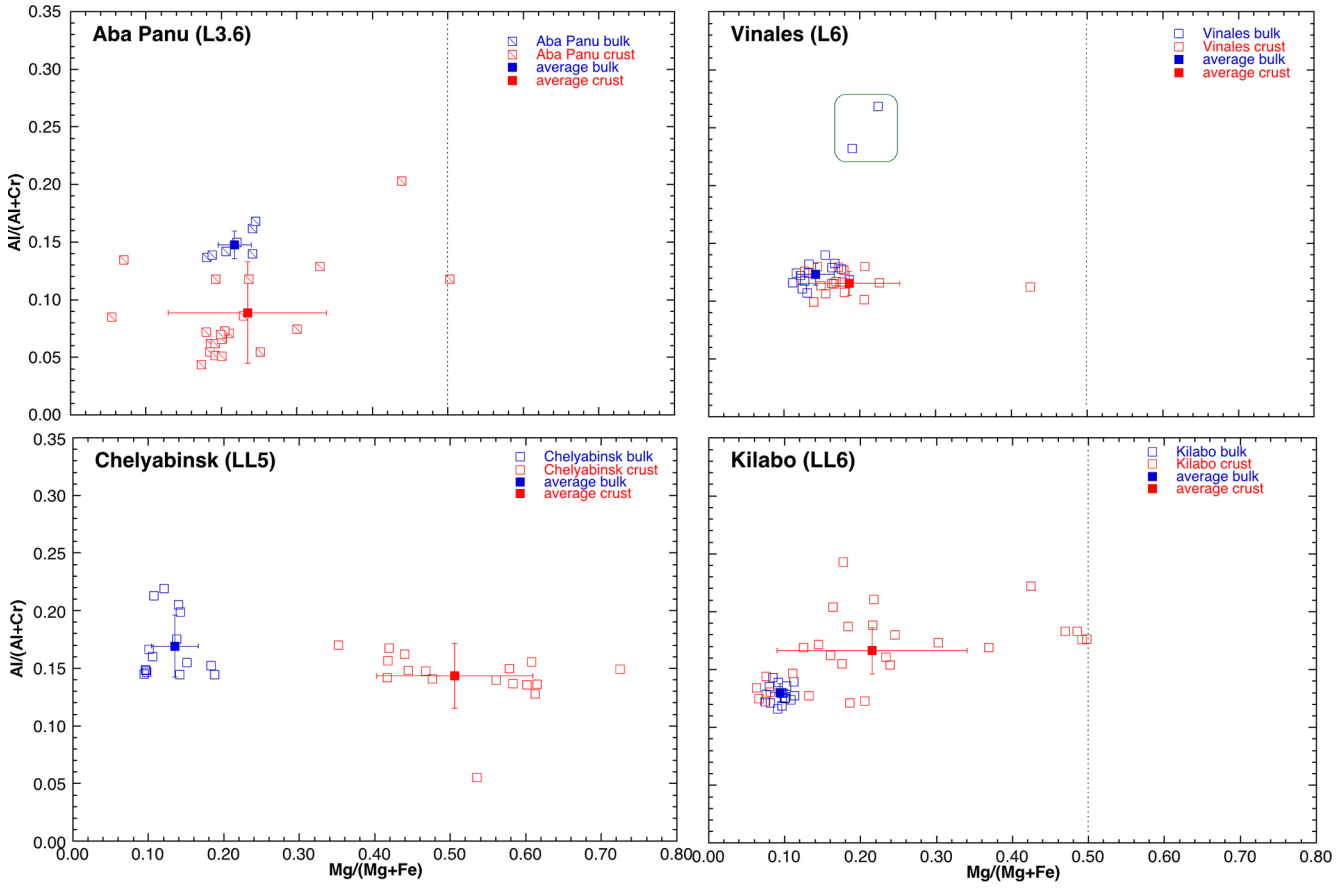

Figure 3. Al/(Al + Cr) vs. Mg/(Mg + Fe) values for chromites in a selection of the L and LL chondrites studied. With the exception of the Aba Panu L3.6 chondrite, the chromites found in the fusion crust (unfilled red symbols) display higher Mg/(Mg + Fe) values; for all samples the standard deviation of the Mg# number is much larger in the crust than in the meteorite interior. Symbols are as in Fig. 2. The chromites enclosed in green (Viñales) are not coarse chromites but small euhedral chromites within a chromite–plagioclase assemblage (Rubin, 2003).

High chemical variability is present considering chromites in the fusion crusts: while Al# is comparable with that determined for the chromites in the interior (between 0.09 and 0.17), Mg# has higher values (and larger standard deviations), sometimes plotting in the Mg-chromite field (Mg# > 0.5).

Rarely, chromites in the fusion crust have a Mg + Fe sum that significantly exceeds 1 (and, correspondingly, an Al + Cr + Ti + V sum significantly lower than 2). A possible explanation is the presence of Fe^{3+} in the octahedral site, thus introducing a small magnetite component into the composition. Nevertheless, SEM data alone can neither confirm nor reject this hypothesis.

In the experiment of Pittarello et al. (2019) the $Fe^{3+}/(Fe^{2+} + Fe^{3+})$ values in the formed glass were between 0.15 and 0.17, consistently with the formation of small amounts of magnetite in the silicate melt. This is further supported by FE-SEM observation, where magnetite dendrites decorate the residual melt in the synthetic fusion crust, and by a significant magnetite component in the chromite eventually formed within a melted portion of a meteorite.

Notably a small but significant fraction of chromites grown in the fusion crust (25 out of 159, or ∼ 16 %) exhibit detectable Ni content, in marked contrast to those found in the bulk (only 3 out of 150, or ∼ 2 %).

The experimentally formed fusion crust replicates features commonly observed in the fusion crusts of many meteorites, including skeletal olivine with concentric zoning, dendritic olivine, euhedral chromite, skeletal magnetite, botryoidal Fe–FeS aggregates and sulfide veins in the outer substrate.

The composition of chromites within the synthetic fusion crust in the El Hammami meteorites is consistent with data from the natural fusion crusts analysed here: the average Mg# of crust chromites (ca. 0.32) is significantly higher than that of bulk chromites (ca. 0.20) with a notably larger standard deviation.

These data clearly suggest that the Mg# of fusion crusts can differ significantly from that of chromites from the mete-

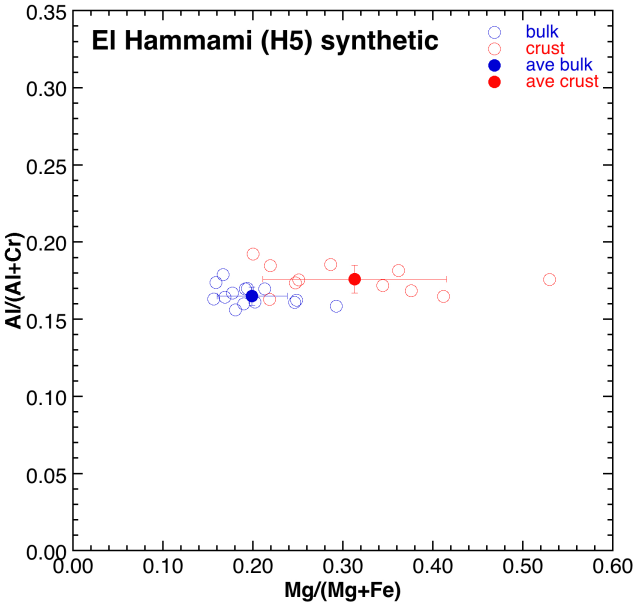

Figure 4. Al/(Al + Cr) vs. Mg/(Mg + Fe) values for chromites in the El Hammami sample experimentally melted by means of an induction-heated plasma wind tunnel. The chromites found in the synthetic fusion crust (unfilled red symbols) display higher Mg/(Mg+Fe) values, as well as a larger standard deviation, consistent with what was found for the natural fusion crust of the ordinary chondrites studied.

orite interior. If so, the Mg/(Mg+Fe) ratio of small chromites in ablation spherules found in the sedimentary record – though valuable for tracing the infall of extraterrestrial material through Earth's history– may be biased and not accurately reflect the composition of the ordinary-chondrite meteoroids from which the ablation spherules originated. For this reason, we suggest using only large-size chromites (possibly representative of bulk chromites) to infer data on meteoroid composition.

Texturally, chromites in the fusion crust have only been found in mesostasis between olivine crystals. Magnetite has always been found in the external portion of the melted crust layer, and in several cases magnetite micro- to nano-crystals mantle chromite crystals (consistent with data from Genge and Grady, 1999, and Genge et al., 2024). We also observed small euhedral to subhedral chromite crystals mantled by magnetite or exhibiting magnetite dendrites at their vertices; however, the reverse (i.e. magnetite mantled by chromite) was never observed. These textural features suggest a crystallisation sequence within the fusion crust: olivine followed by chromite and finally magnetite.

Calculation performed with easyMELTS on the Chelyabinsk and Chergach meteorite compositions suggests that both have a similarly high liquidus temperature (1704 and 1667 °C, respectively). However, the first high-temperature solid phase differs: olivine for Chergach and Cr-spinel for Chelyabinsk. In Chergach, the crystallisation sequence begins with olivine, followed by Cr-spinel, with feldspar and clinopyroxene appearing only at a low residual liquid fraction (ca. 16 %) at around 1000 °C. In contrast, Chelyabinsk exhibits a liquid descent sequence starting with Cr-spinel at 1644 °C, joined by olivine at 1624 °C, and subsequently joined by feldspar and clinopyroxene crystallising at around 1084 °C.

With decreasing temperature in the calculation, spinel composition varies from a chromite-prevalent end-member to magnetite composition. In general, chromite Mg# decreases with temperature, from 0.56 at 1544 °C to 0.13 at 1084 °C in Chergach and from 0.85 at 1644 °C to 0.29 at 1084 °C in Chelyabisk.

5 Conclusions

Chromite in the interiors and corresponding fusion crusts of selected ordinary chondrites – mostly falls, in order to minimise terrestrial weathering effects – and in a synthetic fusion crust produced experimentally via plasma melting of an H5 ordinary chondrite has been investigated.

The chemical data clearly indicate that the Mg# of chromites within the fusion crusts differs significantly from that of chromites in the meteorite interior. This distinction, alongside size and shape, represents an additional criterion to distinguish chromites formed in fusion crust from those in the meteorite interior. Consequently, the Mg/(Mg + Fe) ratio of small-size chromites in ablation spherules found in the sedimentary record may be biased and do not accurately reflect the composition of the source ordinary-chondrite meteoroids. Therefore, when using the chromite compositions to infer meteoroid composition, only larger chromites – potentially representative of the meteorite interior – should be considered.

We regard this work as a preliminary step towards improving the analysis of meteoroid ablation during atmospheric entry, with the aim of enhancing our understanding of ablation spherule formation and of the effects of atmospheric flight on melted micrometeorites.

Code availability. The MELTS code can be accessed at https://magmasource.caltech.edu/alphamelts/ (last access: 18 November 2024; AlphaMELTS DOI: https://doi.org/10.5281/zenodo.13207460, Antoshechkina, 2024).

Data availability. The compositional data are available in the Supplement.

Supplement. The supplement related to this article is available online at https://doi.org/10.5194/ejm-37-617-2025-supplement.

Author contributions. MB: conceptualisation, data curation, investigation; GP: conceptualisation, investigation, review and editing; ADM: data curation, review and editing; SN: conceptualisation, investigation, calculation with easyMELTS, review and editing; LP: conceptualisation, investigation, data curation, review and editing; SG: conceptualisation, investigation, review and editing; CS: conceptualisation, investigation; GG: conceptualisation, data curation, investigation, writing first draft.

Competing interests. The contact author has declared that none of the authors has any competing interests.

Disclaimer. Publisher's note: Copernicus Publications remains neutral with regard to jurisdictional claims made in the text, published maps, institutional affiliations, or any other geographical representation in this paper. While Copernicus Publications makes every effort to include appropriate place names, the final responsibility lies with the authors.

Special issue statement. This article is part of the special issue "Celebrating the outstanding contribution of Paola Bonazzi to mineralogy". It is not associated with a conference.

Acknowledgements. This paper is dedicated to the memory of Paola Bonazzi, with whom we had the fortune of sharing parts of our professional lives. We will always remember her as a passionate and rigorous mineralogist, as well as a wonderful, pleasant woman. We'll miss you.

We greatly acknowledge the editor and the reviewers Alan E. Rubin and Birger Schmitz for their fruitful suggestions.

Financial support. This study was carried out within the Space It Up project funded by the Italian Space Agency, ASI, and the Ministry of University and Research, MUR, under contract no. 2024-5-E.0 – CUP no. I53D24000060005. Steven Goderis acknowledges the support of the VUB Strategic Research Program and thanks the Belgian Science Policy (BELSPO) and the Research Foundation – Flanders (FWO) for funding.

Review statement. This paper was edited by Dmitry Pushcharovsky and reviewed by Alan E. Rubin and Birger Schmitz.

References

Antoshechkina, P.: magmasource/alphaMELTS: v2.3.1, Zenodo [code], https://doi.org/10.5281/zenodo.13207460, 2024.

Bunch, T. E., Keil, K., and Snetsinger, K. G.: Chromite composition in relation to chemistry and texture of ordinary chondrites, Geochim. Cosmochim. Ac., 31, 1569–1582, https://doi.org/10.1016/0016-7037(67)90105-6, 1967.

Genge, M. J. and Grady, M. M.: The fusion crusts of stony meteorites: Implications for the atmospheric reprocessing of extraterrestrial materials, Meteorit. Planet. Sci., 34, 341–356, https://doi.org/10.1111/j.1945-5100.1999.tb01344.x, 1999.

Genge, M. J., Alesbrook, L., Almeida, N. V., Bates, H. C., Bland, P. A., Boyd, M. R., Burchell, M. J., Collins, G. S., Cornwell, L. T., Daly, L., Devillepoix, H. A. R., van Ginneken, M., Greshake, A., Hallatt, D., Hamann, C., Hecht, L., Jenkins, L. E., Johnson, D., Jones, R., King, A. J., Mansour, H., McMullan, S., Mitchell, J. T., Rollinson, G., Russell, S. S., Schröder, C., Stephen, N. R., Suttle, M. D., Tandy, J. D., Trimby, P., Sansom, E. K., Spathis, V., Willcocks, F. M., and Wozniakiewicz, P. J.: The fusion crust of the Winchcombe meteorite: A preserved record of atmospheric entry processes, Meteorit. Planet. Sci., 59, 948–972, https://doi.org/10.1111/maps.13937, 2024.

Ghiorso, M. S. and Sack, R. O.: Chemical mass transfer in magmatic processes IV. A revised and internally consistent thermodynamic model for the interpolation and extrapolation of liquid-solid equilibria in magmatic systems at elevated temperatures and pressures, Contr. Mineral. and Petrol., 119, 197–212, https://doi.org/10.1007/BF00307281, 1995.

Helber, B., Dias, B., Bariselli, F., Zavalan, L. F., Pittarello, L., Goderis, S., Soens, B., McKibbin, S. J., Claeys, P., and Magin, T. E.: Analysis of Meteoroid Ablation Based on Plasma Wind-tunnel Experiments, Surface Characterization, and Numerical Simulations, Astrophys. J., 876, 120, https://doi.org/10.3847/1538-4357/ab16f0, 2019.

Pittarello, L., Goderis, S., Soens, B., McKibbin, S. J., Giuli, G., Bariselli, F., Dias, B., Helberg, B., Lepore, G. O., Vanhaecke, F., Koeberl, C., Magin, T. E., and Claeys, P.: Meteoroid atmospheric entry investigated with plasma flow experiments: Petrography and geochemistry of the recovered material, Icarus, 331, 170–178, https://doi.org/10.1016/j.icarus.2019.04.033, 2019.

Ramdohr, P.: Chromite and chromite chondrules in meteorites, Geochim. Cosmochim. Ac., 31, 1961–1963, https://doi.org/10.1016/0016-7037(67)90135-4, 1967.

Ramdohr, P.: The Opaque Minerals in Stony Meteorites, Elsevier, Amsterdam 245 pp., https://doi.org/10.1017/S0016756800045696, 1973.

Rubin, A. E.: Chromite-plagioclase assemblages as a new shock indicator; Implications for the shock and thermal histories of ordinary chondrites, Geochim. Cosmochim. Ac., 67, 2695–2709, https://doi.org/10.1016/0016-7037(67)90135-4, 2003.

Schmitz, B.: Extraterrestrial spinels and the astronomical perspective on eEarth's geological record and evolution of life, Chemie der Erde, 73, 117–145, https://doi.org/10.1016/j.chemer.2013.04.002, 2013.

Schmitz, B. and Tassinari, M.: Fossil Meteorites, in: Accretion of Extraterrestrial Matter Throughout Earth's History, edited by: Peucker-Ehrenbrink B. and Schmitz B., Springer, Boston, MA., 319–331, https://doi.org/10.1007/978-1-4419-8694-8_17, 2001.

Schmitz, B., Heck, P. R., Alvarez, W., Kita, N. T., Rout, S. S., Cronholm, A., Defouilloy, C., Martin, E., Smit., J., and Terfelt, F.: Meteorite flux to Earth in the early cretaceous as reconstructed from sediment dispersed extraterrestrial spinels, Geology, 45, 807–810, https://doi.org/10.1130/G39297.1, 2017.

Smith, P. M. and Asimow, P. D.: Adiabat_1ph: A new public front-end to the MELTS, pMELTS, and pH-

MELTS models, Geochem. Geophy. Geosy., 6, Q02004, https://doi.org/10.1029/2004GC000816, 2005.
Taylor, S. and Brownlee, D. E.: Cosmic Spherules in the Geologic Record, Meteorit. Planet. Sci., 26, 203–211, 1991.
Wlotzka, F.: Cr spinel and chromite as petrogenetic indicators in ordinary chondrites: Equilibration temperatures of petrologic types 3.7 to 6, Meteorit. Planet. Sci., 40, 1673–1702, https://doi.org/10.1111/j.1945-5100.2005.tb00138.x, 2005.